Amplitude analyses
Part 1

Anton Poluektov

The University of Warwick, UK

13 September 2018

Sorry Sebastien

Introduction

Amplitude analyses: a powerful analysis technique; study of *dynamical* structure of a decay amplitude by analysing *kinematical* distributions of decay products.

Basically, anything beyond fitting invariant mass peaks is an amplitude analysis.

What kind of *dynamical structure* of the amplitude we are taking about?

- Multibody decay $X \to abc\ldots$ almost never occurs in a single point in space.
- There are forces acting between decay products. Can be seen as production of resonant intermediate states: $D \to R_1(\to ab)c\ldots$.
- The same decay can have many intermediate resonant amplitudes that interfere. Amplitude analyses provide information about these interfering components.

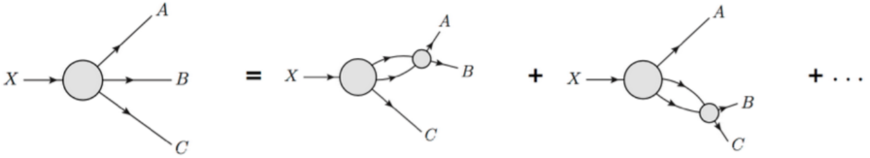

Why is this interesting?

- Search for **New Physics**: if we look for the contributions that give the amplitudes different from SM (e.g. $B \to K^* \mu\mu$, $B \to K\pi\pi\gamma$).
- **Hadron spectroscopy**: study of resonance states themselves (mass, width, spin, parity, etc.), including exotic (e.g. pentaquarks)
- Direct access to **phases** of different components, which can exhibit **CP violation** (e.g. charmless B decays).
- Study of the properties of the initial state X (e.g. X itself can be a quantum superposition of two states; measurements of **CKM angles**, e.g. $D^0 \to$multibody from B decays).

How does one do it technically?

- Typically, one should know the *complex structure* of each of the interfering amplitudes
- The *fit to kinematic distribution* in data gives relative magnitudes and phases between amplitude components.
- There are also other, more *model-independent* ways of doing amplitude analyses (examples later).

Part I
2D: Dalitz plot analyses

Two-body decay kinematics

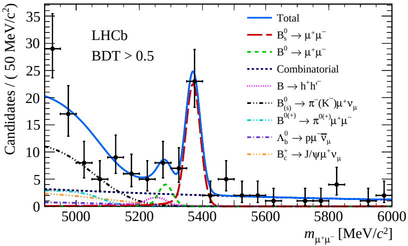

Two-body decay (e.g. $B_s \to \mu^+\mu^-$). Kinematics is completely fixed by conservation laws.

$D \to ab$: in D rest frame decay is isotropic (unless D is non-scalar and is polarised),

$$\vec{p}_a = -\vec{p}_b$$

$$|p_a|^2 = |p_b|^2 = \frac{(M_D^2 - (M_a - M_b)^2)(M_D^2 - (M_a + M_b)^2)}{4M_D^2}$$

[PDG review: Kinematics]

Can measure branching ratios, CP asymmetries, etc., but no access to individual amplitudes.

Three-body decays of scalars: Dalitz plot

Three-body decays $D \to abc$: things are becoming more interesting.

- In D rest frame, all a, b, c lie in the plane (e.g. $p^{(z)}_{a,b,c} \equiv 0$).
- Rotate coordinates such that e.g. $\vec{p}_c = (0, p^{(y)}_c, 0)$.
- Five kinematic observables ($p^{(x)}_a$, $p^{(y)}_a$, $p^{(x)}_b$, $p^{(y)}_b$, $p^{(y)}_c$,), but 3 constraints from kinematics (conservation of momentum in x, y, conservation of energy).
- Two *internal* degrees of freedom remain, fully defined by *dynamics* of the decay. Can take any pair of independent parameters as variables for amplitude parametrization: **Dalitz plot**.
- Most common choice: two pairs of invariant masses squared (e.g. m^2_{ab}, m^2_{bc}).
- 3 pairs are linearly dependent: $m^2_{ab} + m^2_{ac} + m^2_{bc} = M^2_D + M^2_a + M^2_b + M^2_c$

Phase space is uniform in variables m^2_{ab}, m^2_{bc}:

$$d\Gamma = \frac{1}{(2\pi)^3}\frac{1}{32M^3}|\mathcal{A}(m^2_{ab}, m^2_{bc})|^2 dm^2_{ab} dm^2_{bc} \, .$$

Any non-uniformity is due to dynamical properties of amplitude $\mathcal{A}(m^2_{ab}, m^2_{bc})$.

[PDG review: Kinematics]

[Physics of B factories: Dalitz analysis section]

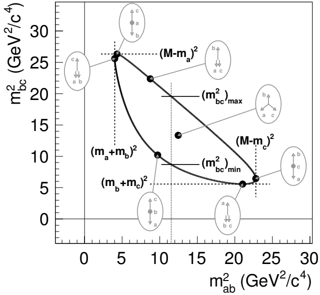

A bit of history: Richard Dalitz and θ/τ puzzle

R. H. Dalitz (1925–2006)

["On the analysis of τ-meson data and the nature of the τ-meson", Phil. Mag. 44 (1953) 1068]

Decays of two strange particles with consistent masses were observed in 1950-s:

- $\theta^+ \to \pi^+\pi^0$: $J^P = 0^+, 1^-, 2^+ \ldots$
- $\tau^+ \to \pi^+\pi^-\pi^+$: $J^P = 0^-, 1^\pm, 2^\pm \ldots$

Is it two different partciles, or one?

R.H. Dalitz: plot in two variables, functions of kinetic energies $T_{1,2,3}$ and $Q = m_\theta - 3m_\pi$:

$$x = \frac{\sqrt{3}(T_1 - T_2)}{Q},$$

$$y = \frac{2T_3 - T_1 - T_2}{Q}$$

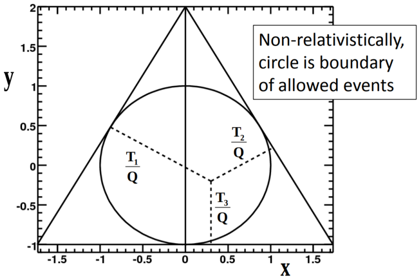

The distributions of events in x, y should depend on J^P of the initial state

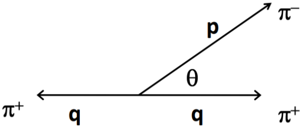

$$
\begin{array}{ll}
J^P = 0^- & 1 \\
J^P = 1^+ & p^2 \\
J^P = 1^- & p^4 q^4 \sin^2\theta \cos^2\theta \\
J^P = 2^+ & p^2 q^4 \sin^2\theta
\end{array}
$$

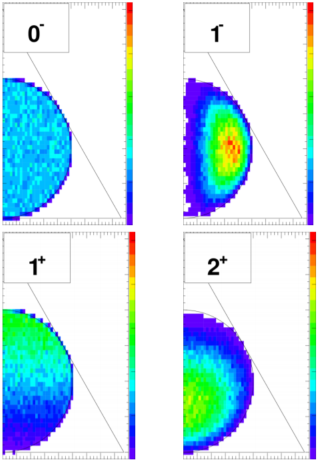

A bit of history: Richard Dalitz and θ/τ puzzle

The data is consistent with $J^P = 0^-$ for τ^+

But $\theta^+ \to \pi^+\pi^0$ cannot have $J^P = 0^-$!

Why two different particles with the same mass?

Solution (C.S. Wu *et al.*, 1957):
parity violation in weak interaction
(β decay of ^{60}Co)

Now, θ^+ and τ^+ are known as charged kaon.

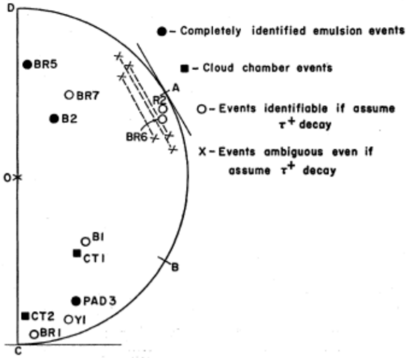

FIG. 3. The data on τ-meson decay events in which the signs of π-meson charges are established.

Consider quasi-two-body amplitude in three-body decays: $D \to AR(\to BC)$

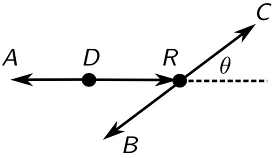

Take the angle θ between the R direction in D rest frame, and BC direction in R rest frame.

θ is Lorentz-invariant and can be expressed as a function of Dalitz plot variables.

$$\cos\theta = \frac{M^2_{ab} - M^2_{ab,min}}{M^2_{ab,max} - M^2_{ab,min}}$$

Distribution of θ depends on the spin of the intermediate state R. Legendre polynomial $P_J(x)$; $\mathcal{A} \propto P_J(\cos\theta)$

$J = 0$	$\mathcal{A}(x) = 1$
$J = 1$	$\mathcal{A}(x) = x$
$J = 2$	$\mathcal{A}(x) = \frac{1}{2}(3x^2 - 1)$
$J = 3$	$\mathcal{A}(x) = \frac{1}{2}(5x^3 - 3x)$

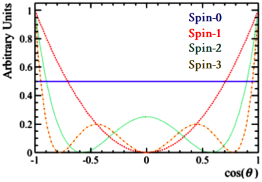

The density is of course $p(\cos\theta) \propto |\mathcal{A}(\cos\theta)|^2$.

Consider quasi-two-body amplitude in three-body decays: $D \to AR(\to BC)$

The distribution in another Dalitz plot variable, M^2_{BC}, is now defined by the *dynamics* of the decay.

- This is a much more difficult question; most of the uncertainty in current measurements is due to lineshape parametrisation.
- Many models are on market. Still a lot of development.
- Model-independent approaches can be used sometimes.

Single narrow ($\Gamma_R \ll M_R$) resonance: Breit-Wigner parametrisation.

In any other cases (several overlapping resonances with the same quantum numbers, wide resonance with $\Gamma \simeq M$) the BW parametrisation is, strictly speaking, not physical. Nevertheless, it is often used and gives reasonable results.

(more about this later)

Lineshapes; Breit-Wigner amplitude

Single narrow ($\Gamma_R \ll M_R$) resonance: Breit-Wigner parametrisation

$$\mathcal{A}_{BW} = \frac{1}{M_R^2 - M_{MC}^2 - iM_R\Gamma_R}$$

"Argand plot"

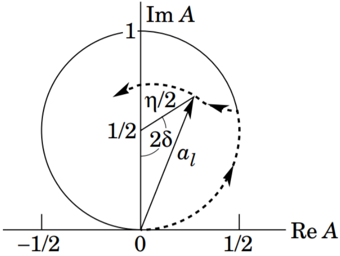

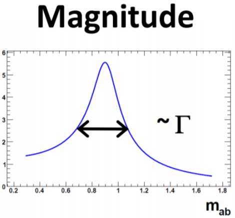

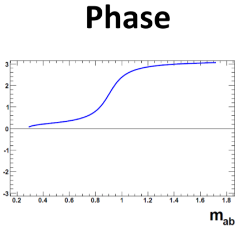

Counter-clockwise rotation of the phase with increasing M_{bc}^2.

Essential: *e.g.* clockwise rotation would correspond to complex-conjugate BW amplitude, which is unphysical.

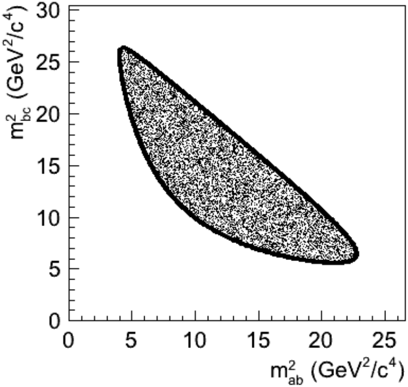

- Phase-space decay
- Scalar in *ab* channel
- Scalar in *bc* channel
- Scalar in *ac* channel
- Vector in *ab* channel
- Tensor ($J = 2$) in *ab* channel
- Two scalars in *ab* and *bc* channels, $\Delta\phi = 0^\circ$
- Two scalars in *ab* and *bc* channels, $\Delta\phi = 90^\circ$
- Two scalars in *ab* and *bc* channels, $\Delta\phi = 180^\circ$
- Scalar and vector in *ab* channel, $\Delta\phi = 0^\circ$

Resonances on the Dalitz plot

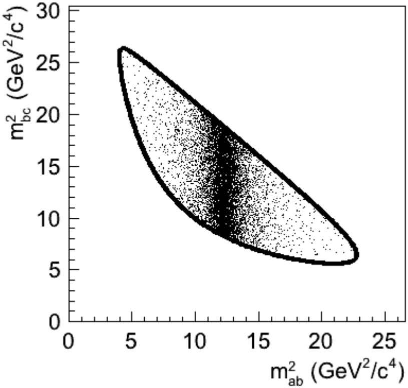

- Phase-space decay
- Scalar in *ab* channel
- Scalar in *bc* channel
- Scalar in *ac* channel
- Vector in *ab* channel
- Tensor ($J = 2$) in *ab* channel
- Two scalars in *ab* and *bc* channels, $\Delta\phi = 0^\circ$
- Two scalars in *ab* and *bc* channels, $\Delta\phi = 90^\circ$
- Two scalars in *ab* and *bc* channels, $\Delta\phi = 180^\circ$
- Scalar and vector in *ab* channel, $\Delta\phi = 0^\circ$

Resonances on the Dalitz plot

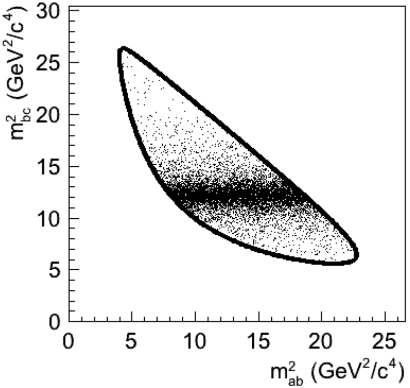

- Phase-space decay
- Scalar in *ab* channel
- Scalar in *bc* channel
- Scalar in *ac* channel
- Vector in *ab* channel
- Tensor ($J = 2$) in *ab* channel
- Two scalars in *ab* and *bc* channels, $\Delta\phi = 0^\circ$
- Two scalars in *ab* and *bc* channels, $\Delta\phi = 90^\circ$
- Two scalars in *ab* and *bc* channels, $\Delta\phi = 180^\circ$
- Scalar and vector in *ab* channel, $\Delta\phi = 0^\circ$

Resonances on the Dalitz plot

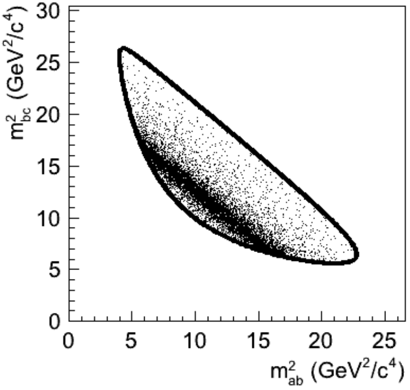

- Phase-space decay
- Scalar in *ab* channel
- Scalar in *bc* channel
- Scalar in *ac* channel
- Vector in *ab* channel
- Tensor ($J = 2$) in *ab* channel
- Two scalars in *ab* and *bc* channels, $\Delta\phi = 0^\circ$
- Two scalars in *ab* and *bc* channels, $\Delta\phi = 90^\circ$
- Two scalars in *ab* and *bc* channels, $\Delta\phi = 180^\circ$
- Scalar and vector in *ab* channel, $\Delta\phi = 0^\circ$

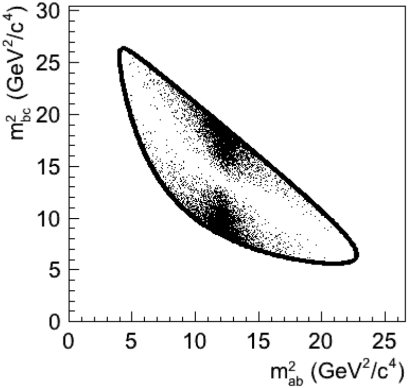

- Phase-space decay
- Scalar in *ab* channel
- Scalar in *bc* channel
- Scalar in *ac* channel
- Vector in *ab* channel
- Tensor ($J = 2$) in *ab* channel
- Two scalars in *ab* and *bc* channels, $\Delta\phi = 0^\circ$
- Two scalars in *ab* and *bc* channels, $\Delta\phi = 90^\circ$
- Two scalars in *ab* and *bc* channels, $\Delta\phi = 180^\circ$
- Scalar and vector in *ab* channel, $\Delta\phi = 0^\circ$

Resonances on the Dalitz plot

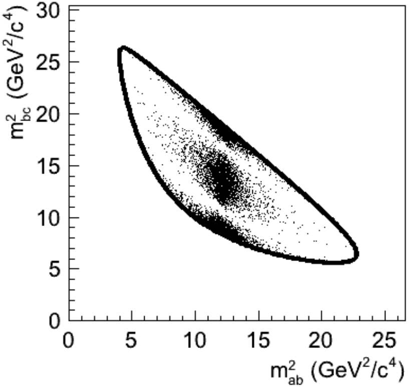

- Phase-space decay
- Scalar in *ab* channel
- Scalar in *bc* channel
- Scalar in *ac* channel
- Vector in *ab* channel
- Tensor ($J = 2$) in *ab* channel
- Two scalars in *ab* and *bc* channels, $\Delta\phi = 0^\circ$
- Two scalars in *ab* and *bc* channels, $\Delta\phi = 90^\circ$
- Two scalars in *ab* and *bc* channels, $\Delta\phi = 180^\circ$
- Scalar and vector in *ab* channel, $\Delta\phi = 0^\circ$

Resonances on the Dalitz plot

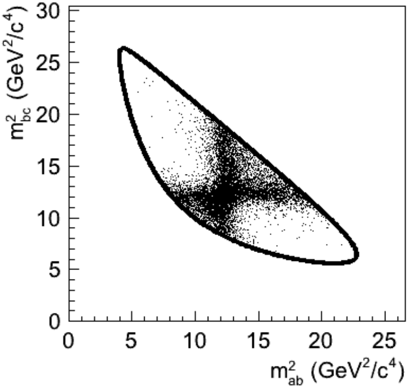

- Phase-space decay
- Scalar in *ab* channel
- Scalar in *bc* channel
- Scalar in *ac* channel
- Vector in *ab* channel
- Tensor ($J = 2$) in *ab* channel
- Two scalars in *ab* and *bc* channels, $\Delta\phi = 0^\circ$
- Two scalars in *ab* and *bc* channels, $\Delta\phi = 90^\circ$
- Two scalars in *ab* and *bc* channels, $\Delta\phi = 180^\circ$
- Scalar and vector in *ab* channel, $\Delta\phi = 0^\circ$

Resonances on the Dalitz plot

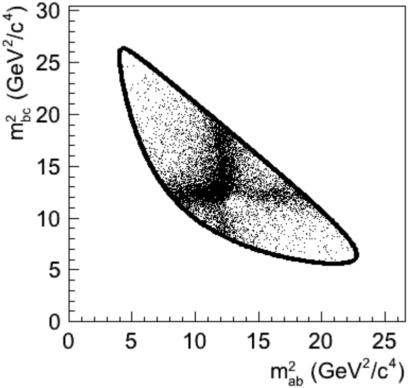

- Phase-space decay
- Scalar in *ab* channel
- Scalar in *bc* channel
- Scalar in *ac* channel
- Vector in *ab* channel
- Tensor ($J = 2$) in *ab* channel
- Two scalars in *ab* and *bc* channels, $\Delta\phi = 0^\circ$
- Two scalars in *ab* and *bc* channels, $\Delta\phi = 90^\circ$
- Two scalars in *ab* and *bc* channels, $\Delta\phi = 180^\circ$
- Scalar and vector in *ab* channel, $\Delta\phi = 0^\circ$

Resonances on the Dalitz plot

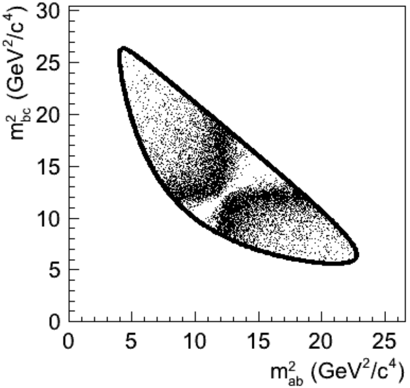

- Phase-space decay
- Scalar in *ab* channel
- Scalar in *bc* channel
- Scalar in *ac* channel
- Vector in *ab* channel
- Tensor ($J = 2$) in *ab* channel
- Two scalars in *ab* and *bc* channels, $\Delta\phi = 0^\circ$
- Two scalars in *ab* and *bc* channels, $\Delta\phi = 90^\circ$
- Two scalars in *ab* and *bc* channels, $\Delta\phi = 180^\circ$
- Scalar and vector in *ab* channel, $\Delta\phi = 0^\circ$

Resonances on the Dalitz plot

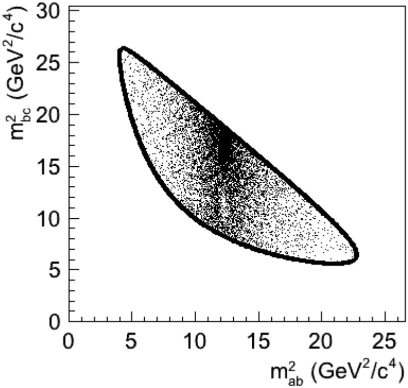

- Phase-space decay
- Scalar in *ab* channel
- Scalar in *bc* channel
- Scalar in *ac* channel
- Vector in *ab* channel
- Tensor ($J = 2$) in *ab* channel
- Two scalars in *ab* and *bc* channels, $\Delta\phi = 0^\circ$
- Two scalars in *ab* and *bc* channels, $\Delta\phi = 90^\circ$
- Two scalars in *ab* and *bc* channels, $\Delta\phi = 180^\circ$
- Scalar and vector in *ab* channel, $\Delta\phi = 0^\circ$

Three-body decays on the Dalitz plot

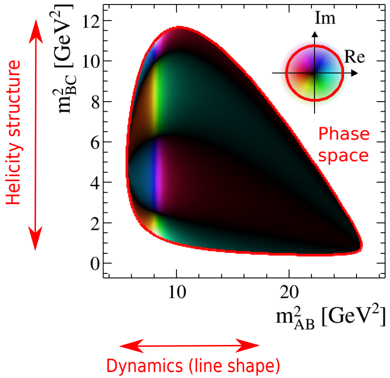

- Absolute phase not visible, but phases of components can be accessed though interference with other structures.
- Model-dependent fits: typically isobar model (sum of resonant/nonresonant components)
- Semi-model-independent fits: describe some partial waves as complex bins/splines, determine amplitude and phase through interference with other components.
- Model-independent partial wave analysis (PWA): for spin J, polynomials up to $2J$ order. Helicity as a function of M^2_{AB}.

Three-body decays on the Dalitz plot

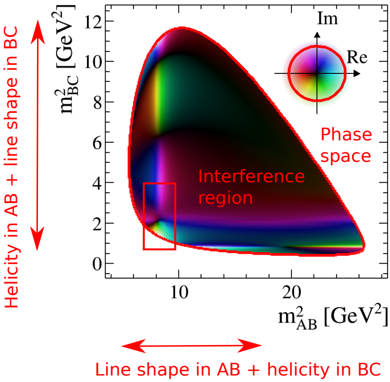

- Absolute phase not visible, but phases of components can be accessed though interference with other structures.
- Model-dependent fits: typically isobar model (sum of resonant/nonresonant components)
- Semi-model-independent fits: describe some partial waves as complex bins/splines, determine amplitude and phase through interference with other components.
- Model-independent partial wave analysis (PWA): for spin J, polynomials up to $2J$ order. Helicity as a function of M^2_{AB}.

Most of current analyses treat the 3-body (or n-body amplitude) as a coherent sum of quasi-two-body amplitudes in different channels (ab, bc, ac for 3-body):

$$\begin{aligned}\mathcal{A} = &\sum_i C_i R_i^{(ab)}(m^2_{ab}) T_i^{(ab)}(\theta_{ab}) + \\ &\sum_j C_j R_i^{(bc)}(m^2_{bc}) T_i^{(bc)}(\theta_{cb}) + \\ &\sum_k C_k R_i^{(ac)}(m^2_{ac}) T_i^{(ac)}(\theta_{ac})\end{aligned}$$

This is called **isobar model**.

The density $p(m^2_{ab}, m^2_{bc}) = |\mathcal{A}(m^2_{ab}, m^2_{bc})|^2$ is fitted to density of events in data (after accounting for background and non-uniform efficiency).

Typically, complex amplitudes $C_{i,j,k}$ are free parameters in the fit. as can be some of resonance parameters (masses, widths of not-so-well-known resonances).

Many more variations of this scheme are possible, some of which will be illustrated later.

Spin formalisms

You will see different expressions for angular terms in the literature:

Helicity formalism: angular distribution as a function of helicity angle $\theta(m_{bc})$

$$M_1 = \cos\theta$$

$$M_2 = \cos^2\theta - \frac{1}{3}$$

Zemach tensors: expressions involving 3-momenta

$$M_1 = -2\vec{p}\cdot\vec{q}$$

$$M_2 = \frac{4}{3}[3(\vec{p}\cdot\vec{q}))^2 - (|\vec{p}||\vec{q}|)^2]$$

Both formalisms lead to the same angular distributions $T_J(m^2_{bc})$.

But not fully equivalent: modify lineshapes $R(m^2_{ab})$.

- Centrifugal term q^L (where q is the breakup momentum): should be artificially included in $R(m^2_{ab})$ for helicity formalism to match Zemach tensors.

Fully covariant formalism possible: will be discussed later.

Breit-Wigner resonant shape with various corrections

$$R(m_{ab}^2) = \frac{F_R(\vec{q})F_D(\vec{p})}{(m_0^2 - m_{ab}^2) - im_0\Gamma(m)}$$

Mass-dependent width $\Gamma(M)$:

$$\Gamma(M) = \Gamma_0 \left[\frac{p(M)}{p_0}\right]^{2L_R+1} \frac{m_R}{M} F_R^2(M, L_R),$$

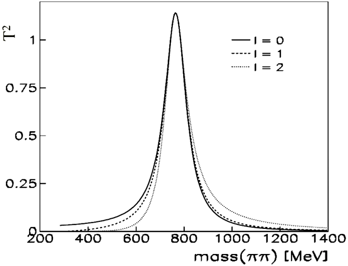

Blatt-Weisskopf centrifugal barrier factors F_i. Take into account the non-pointlike nature of resonance R and decaying particle D, respectively.

$$F_{R,D}(M, L) = \begin{cases} 1 & L = 0 \\ \sqrt{\frac{1+z_0^2}{1+z^2(M)}} & L = 1 \\ \sqrt{\frac{9+3z_0^2+z_0^4}{9+3z^2(M)+z^4(M)}} & L = 2 \end{cases}$$

Where $z(M) = p(M)d$ and $z_0 = p(M_R)d$, and d is the radial parameter (typically, a few GeV^{-1}).

In many cases, amplitude fits require wide slowly-varying amplitude. Not very physical, but can be due to

- Effective parametrisation of some unknown states with small stats (not sufficient to reveal detailed structures)
- Contributions from resonances outside kinematic boundaries

"Non-resonant" shapes

- Charm decays (relatively small phase space): often a constant term is sufficient
- Beauty decays, especially charmless: more sophisticated models are in use.

$$R(m_{ab}^2) = \exp(-\alpha m_{ab}^2)$$

or more advanced ones (LASS, kappa, "dabba" etc.)

Line shapes: K-matrix

Sum of Breit-Wigners with the same quantum numbers violates unitarity.

K-Matrix: ensure unitarity of the amplitude by construction.
Unitarity (= conservation of probability of the scattering process) only makes sense when all available channels are involved. E.g. the amplitude in $\pi^+\pi^-$ channel will depend on the resonances in K^+K^- channel (rescattering!).

$$A_i(s) = (I - iK(s)\rho(s))^{-1}_{ij} P_j(s)$$

where i, j are channel indices (e.g. $\pi\pi$, KK, 4π, $\eta\eta$, etc.), $\rho(s)$ is phase space factor.
Resonances correspond to poles of the K-matrix. Parametrisation:

$$K_{ij}(s) = \left(\sum_\alpha \frac{g_i^\alpha g_j^\alpha}{m_\alpha^2 - s} + f_{ij}^{\mathrm{scatt}} \frac{1 - s_0^{\mathrm{scatt}}}{s - s_0^{\mathrm{scatt}}} \right) f_{A0}(s)$$

Parameters of K-matrix (pole couplings g and scattering amplitudes f) are taken from the global analysis of $\pi^+\pi^-$ ($p\pi^-$) scattering data.
Production vector has the same poles as K matrix

$$P_i(s) = \sum_\alpha \frac{\beta_\alpha g_i^\alpha}{m_\alpha^2 - s} + f_{1i}^{\mathrm{prod}} \frac{1 - s_0^{\mathrm{prod}}}{s - s_0^{\mathrm{prod}}}$$

Parameters β, f depend on production mechanism and are fit parameters.

Flatté: a particular case of K-matrix with only one pole and two channels. Useful if 2nd channels opens near the resonance mass (e.g. for $f_0(980) \to \pi\pi$ to account for rescattering from KK)

$$R(m_{ab}^2) = \frac{1}{m_0^2 - m_{ab}^2 - i m_0 (g_1 \rho_1(m_{ab}^2) + g_2 \rho_2(m_{ab}^2))}$$

K-matrix if not a silver bullet: while preserving unitarity it violates analyticity (phase-space term).

There are formalisms that attempt to preserve both, but these are very expensive computationally.
[JPAC]: collaboration of theorists and experimentalists aims to solve this eventually

---

Kinematical effects in rescattering can lead to structures that can resemble resonances

Cusps: rescattering without binding.
[E.S.Swanson, Phys. Rev. D91 034009, 2015]

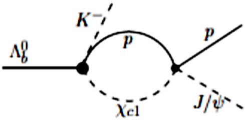

$B \to$ charmless decays: very large phase space, resonances concentrate near the edges
Modified phase space magnifying interference regions, mass vs. helicity angle

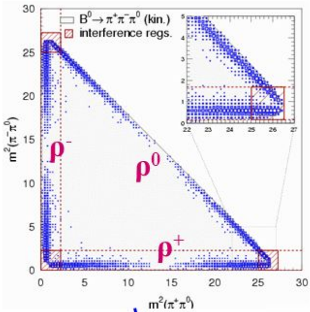

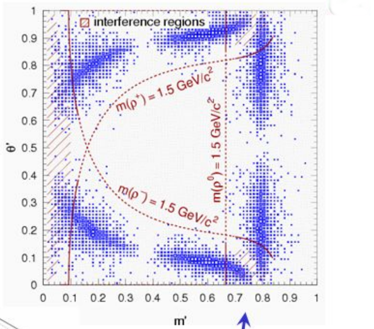

Jacobian

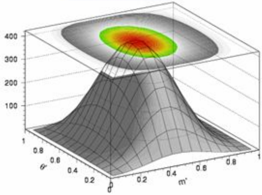

$$\theta' = \frac{1}{\pi}\cos^{-1}(\cos\theta_{+-})$$
$$m' = \frac{1}{\pi}\cos^{-1}\left[2\frac{m_{+-} - m_{+-}^{\min}}{m_{+-}^{\max} - m_{+-}^{\min}} - 1\right]$$

"blow up" ρ bands & interference regions

[BaBar collaboration, PRD72 052002 (2005)]

Dalitz plot analyses: signal selection

Amplitude analyses generally require sufficiently clean selection (uncertainty due to background)

"Standard " figures of merit for selection optimisation ($S/\sqrt{S+B}$) are not well motivated.

[[PRL 112 (2014) 011801]]

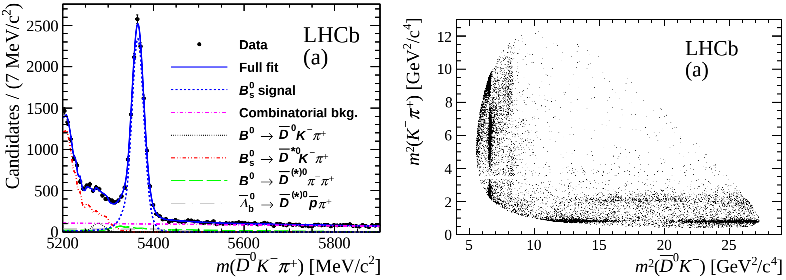

Selection window $|M(DK\pi) - M(B_s)| < X$.

Uncorrected invariant masses would result in fuzzy Dalitz plot (different $M(DK\pi)$ give somewhat different phase space).

Kinematic fit to constrain $M(DK\pi)$ to be equal to $M(B_s)$.

Dalitz plot analyses: unbinned fit

Minimise the unbinned negative logarithmic likelihood:

$$-2\ln\mathcal{L} = -2\sum_{i=1}^{N}\ln p_{\mathrm{tot}}(x_i),$$

Where x_i is a (vector of) data points, $p_{\mathrm{tot}}(x)$ is normalised total density:

$$p_{\mathrm{tot}}(x) = p(x)\epsilon(x)\frac{n_{\mathrm{sig}}}{\mathcal{N}} + p_{\mathrm{bck}}(x)\frac{n_{\mathrm{bck}}}{\mathcal{N}_{\mathrm{bck}}},$$

Signal and background normalisations:

$$\mathcal{N} = \int_{\mathcal{D}} p(x)\epsilon(x)\,dx, \qquad \mathcal{N}_{\mathrm{bck}} = \int_{\mathcal{D}} p_{\mathrm{bck}}(x)\,dx,$$

Normalisation has to be recalculated at every minimisation step: computationally heavy.
Trick that works if only C_i are floating: expand the normalisation as

$$\mathcal{N} = \sum_{i,j}\left[C_i C_j^* \int_{\mathcal{D}} Re(\mathcal{A}_i(x)\mathcal{A}_j^*(x))dx\right]$$

where the integrals have to be calculated only once.

Dalitz plot analyses: acceptance effects

Efficiency over the Dalitz plot is not uniform because of detector acceptance and selection requirements.

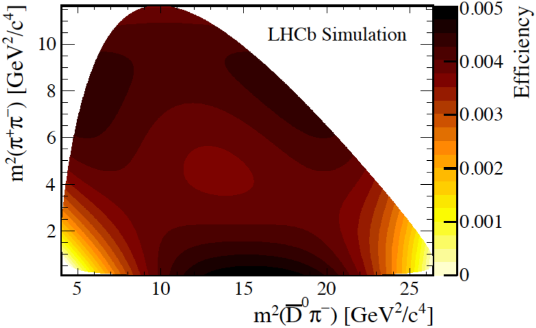

Typically obtained from full simulation. Various choices to parametrise the shape:

- Histogram
- Polynomials
- Kernel density (with edge correction)

Dalitz plot analyses: acceptance effects

Non-uniform **efficiency** can be handled by including the scattered data from simulation directly into the likelihood normalisation term
Apply MC integration for normalisation term (forget about background for simplicity):

$$-2\ln\mathcal{L} = -2\sum_{i=1}^{N}\ln p(x_i)\epsilon(x_i)/\mathcal{N} = -2\sum_{i=1}^{N}\ln p(x_i) - 2\sum_{i=1}^{N}\ln\epsilon(x_i) + 2N\ln\sum_{j=1}^{M}p(y_j)\epsilon(y_j)$$

y_j are uniformly distributed normalisation points. Forget about constant term:

$$-2\ln\mathcal{L} = -2\sum_{i=1}^{N}\ln p(x_i) + 2N\ln\sum_{j=1}^{M}p(y_j)\epsilon(y_j)$$

Can see 2nd term as sum over uniform events each entering with weight $\epsilon(y_i)$.

Equivalent: can take the sum over non-uniform sample of events obtained from the uniform sample y_i which passed the detector acceptance with probability $\epsilon(y_j)$. $\Rightarrow$ do not need to parametrise $\epsilon(x)$!

Dalitz plot analyses: backgrounds

Two approaches to handle **background**:

cFit: Needs explicit background parametrisation (e.g. data from sidebands)

- Could be difficult for multidimensional fits
- Additional systematics due to parametrisation

sFit: Statistical subtraction of the background from the sideband distribution using sWeight technique [M. Pivk and F. Le Diberder, NIM A555, 356–369 (2005)]

- Each event is given a weight w_i (calculated from signal/background discriminating distribution, e.g. B mass), negative for background-like and positive for signal-like events.
- The weight w_i enters each data term in the likelihood:
  $$-2\sum_{i=1}^{N}\ln p(x_i) \quad \to \quad -2\sum_{i=1}^{N} w_i \ln p(x_i)$$
- Statistically subtract background. Functional parametrisation of the background is not needed.
- Assumes no correlation between the fitted distribution and the discriminating distribution (inv. mass of the mother particle)
- Larger stat. uncertainty in case of high background

- Finite momentum resolution results in finite resolution in Dalitz variables.
- After the kinematic fit $M(abc) \equiv M_D$ the resolution of m^2_{ab}, m^2_{bc} will be non-uniform (better near the edges, worse in the center of Dalitz plot). Needs MC study.
- Can often be ignored if the amplitude contains only amplitudes with $\Gamma \gg \sigma(m)$. Otherwise, have to numerically convolve $|A|^2$ with the resolution function.

Dalitz plot analyses: reporting results

Fit results expressed in terms of complex couplings C_i depend on the details of the formalism used. Not always easy to reproduce.

- Fit fractions:

$$FF_i = \frac{\int\limits_{\mathcal{D}} |C_i \mathcal{A}_i|^2 d\mathcal{D}}{\int\limits_{\mathcal{D}} |\sum\limits_i C_i \mathcal{A}_i|^2 d\mathcal{D}}$$

- Interference fit fractions:

$$IF_{ij} = \frac{\int\limits_{\mathcal{D}} Re(C_i C_j^* \mathcal{A}_i \mathcal{A}_j^*) d\mathcal{D}}{\int\limits_{\mathcal{D}} |\sum\limits_i C_i \mathcal{A}_i|^2 d\mathcal{D}}$$

Note that $\sum\limits_i FF_i \neq 100\%$ due to interference.

Rather, $\sum\limits_i FF_i + \sum\limits_{i \neq j} IF_{ij} = 100\%$

IF_{ij} between states with different quantum numbers should be zero (orthogonality!)

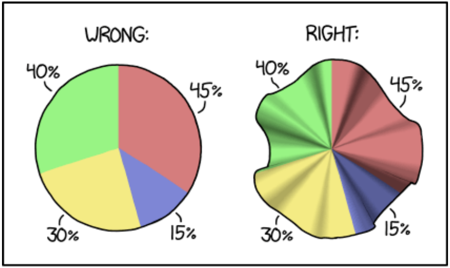

HOW TO MAKE A PIE CHART IF YOUR PERCENTAGES DON'T ADD UP TO 100

Evaluating fit quality

Log. likelihood $-2\ln\mathcal{L}$ does not provide the absolute measure of fit quality.

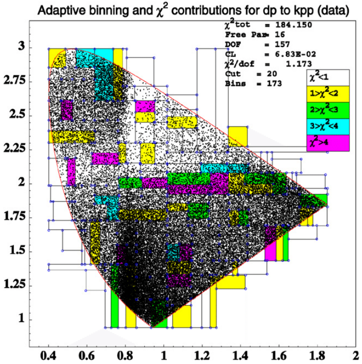

Binned χ^2:

- If the Dalitz plot distribution is very non-uniform, adaptive binning ($\sim$ equal population in bins)
- Calculate χ^2/ndf and its probability.
- However, ndf is not well defined: $ndf = N_{\text{bins}} - N_{\text{pars}}$ is underestimation because the parameters are obtained from an unbinned fit.

Calculate *effective ndf* using toy MC:

- Generate many toy datasets from the fitted amplitude
- Calculate binned χ^2 for each of them.
- Choose ndf_{eff} such that the distribution of $p(\chi^2, ndf_{\text{eff}})$ is uniform (exact coverage).
- Typically $N_{\text{bins}} - N_{\text{pars}} \leq ndf_{\text{eff}} \leq N_{\text{bins}}$

There are unbinned goodness-of-fit test as well:

[M. Williams, JINST 5:P09004 (2010)]

Choice of intermediate resonances

- Adding more terms to the likelihood will describe the given dataset better.
- Adding too much complexity to the model reduces predictive power

How do we balance this? LASSO procedure:

$$-2\ln\mathcal{L} \quad\rightarrow\quad -2\ln\mathcal{L} + \lambda\sum_i\sqrt{\int|C_i\mathcal{A}_i(\mathcal{D})|^2 d\mathcal{D}}$$

Penalise log likelihood by the term proportional to $\sum\sqrt{FF_i}$.

Recipes to choose reasonable values of λ exist (keywords: Akaike and Bayesian information criteria).

Choose λ which minimises

$$AIC(\lambda) = -2\ln\mathcal{L} + 2r,\quad BIC(\lambda) = -2\ln\mathcal{L} + r\ln n$$

r — number of amplitudes over certain threshold
n — number of events in dataset

[Model selection for amplitude analysis, B. Guegan, j. Hardin, J. Stevens, M. Williams]

Amplitude analysis frameworks

Amplitude fits involve a lot of complicated calculations. Several frameworks are available to simplify the task. In many cases, modern parallel architectures (multithreading, GPU) can be used to optimise calculations.

- **Laura++**
  - A powerful tool for traditional 2D Dalitz plot analyses (including time-dependent)
  - Single-threaded, but many clever optimisations
- **MINT**
  - Can do 3-body as well as 4-body final states
- **GooFit**
  - GPU-based fitter, able to do amplitude fits.
- **AmpGen**
  - Just-in-time compiler for amplitudes
  - Can generate code for GooFit
- **Ipanema-β**
  - GPU-based, `python` interface (`pyCUDA`)
- **qft++**
  - Not a fitter itself, but a tool to operate with covariant tensors (used internally by MINT)
- **TensorFlowAnalysis**
  - Set of functions to make amplitude fits and MC generation in Google TensorFlow.
  - Python interface, generates code for multithreaded CPU/GPU.

... and a lot of private analysis-specific code.

[[PRL 112 (2014) 011801]]

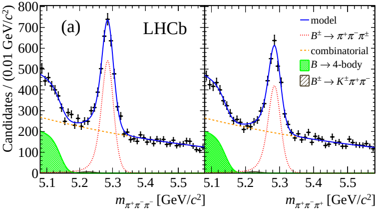

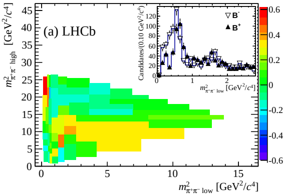

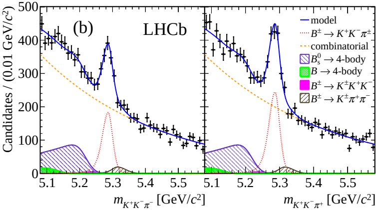

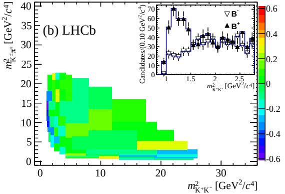

Integrated asymmetries:

$$A_{CP}(B^{\pm} \to \pi^{\pm}\pi^{+}\pi^{-}) = +0.117 \pm 0.021 \pm 0.009 \pm 0.007(J/\psi K^{+})$$
$$A_{CP}(B^{\pm} \to \pi^{\pm}K^{+}K^{-}) = -0.141 \pm 0.040 \pm 0.018 \pm 0.007(J/\psi K^{+})$$

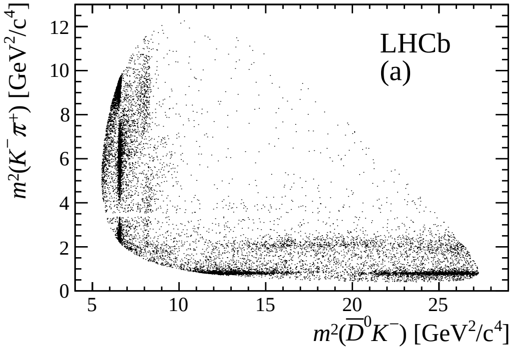

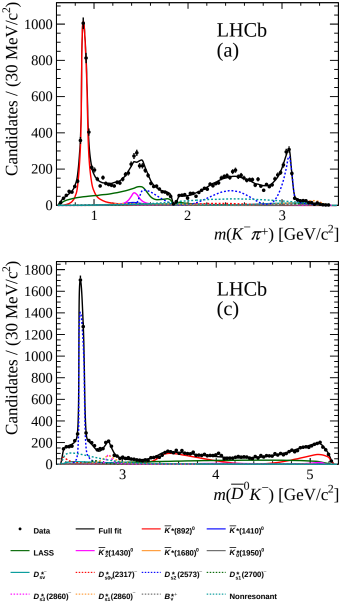

Resonance	Spin	Dalitz plot axis	Model	Parameters (MeV/c^2)
$\overline{K}^*(892)^0$	1	$m^2(K^-\pi^+)$	RBW	$m_0 = 895.81 \pm 0.19$, $\Gamma_0 = 47.4 \pm 0.6$
$\overline{K}^*(1410)^0$	1	$m^2(K^-\pi^+)$	RBW	$m_0 = 1414 \pm 15$, $\Gamma_0 = 232 \pm 21$
$\overline{K}_0^*(1430)^0$	0	$m^2(K^-\pi^+)$	LASS	See text
$\overline{K}_2^*(1430)^0$	2	$m^2(K^-\pi^+)$	RBW	$m_0 = 1432.4 \pm 1.3$, $\Gamma_0 = 109 \pm 5$
$\overline{K}^*(1680)^0$	1	$m^2(K^-\pi^+)$	RBW	$m_0 = 1717 \pm 27$, $\Gamma_0 = 322 \pm 110$
$\overline{K}_0^*(1950)^0$	0	$m^2(K^-\pi^+)$	RBW	$m_0 = 1945 \pm 22$, $\Gamma_0 = 201 \pm 90$
$D_{s2}^*(2573)^-$	2	$m^2(\overline{D}^0K^-)$	RBW	See text
$D_{s1}^*(2700)^-$	1	$m^2(\overline{D}^0K^-)$	RBW	$m_0 = 2709 \pm 4$, $\Gamma_0 = 117 \pm 13$
$D_{sJ}^*(2860)^-$	1	$m^2(\overline{D}^0K^-)$	RBW	See text
$D_{sJ}^*(2860)^-$	3	$m^2(\overline{D}^0K^-)$	RBW	See text
Nonresonant		$m^2(\overline{D}^0K^-)$	EFF	See text
$D_{s\,v}^{*-}$	1	$m^2(\overline{D}^0K^-)$	RBW	$m_0 = 2112.3 \pm 0.5$, $\Gamma_0 = 1.9$
$D_{s0\,v}^*(2317)^-$	0	$m^2(\overline{D}^0K^-)$	RBW	$m_0 = 2317.8 \pm 0.6$, $\Gamma_0 = 3.8$
B_v^{*+}	1	$m^2(\overline{D}^0\pi^+)$	RBW	$m_0 = 5325.2 \pm 0.4$, $\Gamma_0 = 0$

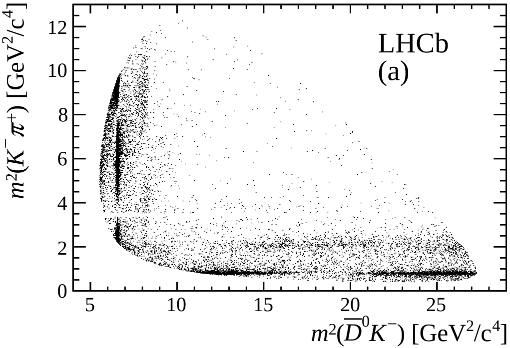

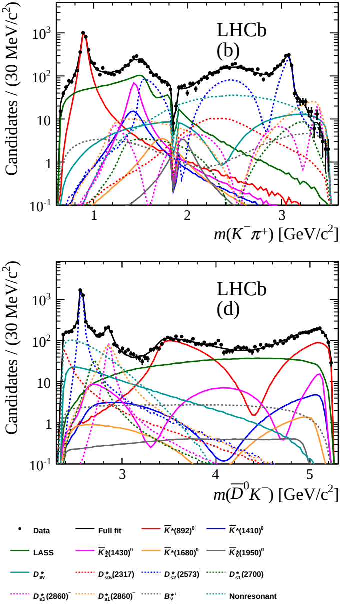

Resonance	Spin	Dalitz plot axis	Model	Parameters (MeV/c^2)
$\bar{K}^*(892)^0$	1	$m^2(K^-\pi^+)$	RBW	$m_0 = 895.81 \pm 0.19$, $\Gamma_0 = 47.4 \pm 0.6$
$\bar{K}^*(1410)^0$	1	$m^2(K^-\pi^+)$	RBW	$m_0 = 1414 \pm 15$, $\Gamma_0 = 232 \pm 21$
$\bar{K}_0^*(1430)^0$	0	$m^2(K^-\pi^+)$	LASS	See text
$\bar{K}_2^*(1430)^0$	2	$m^2(K^-\pi^+)$	RBW	$m_0 = 1432.4 \pm 1.3$, $\Gamma_0 = 109 \pm 5$
$\bar{K}^*(1680)^0$	1	$m^2(K^-\pi^+)$	RBW	$m_0 = 1717 \pm 27$, $\Gamma_0 = 322 \pm 110$
$\bar{K}_0^*(1950)^0$	0	$m^2(K^-\pi^+)$	RBW	$m_0 = 1945 \pm 22$, $\Gamma_0 = 201 \pm 90$
$D_{s2}^*(2573)^-$	2	$m^2(\bar{D}^0K^-)$	RBW	See text
$D_{s1}^*(2700)^-$	1	$m^2(\bar{D}^0K^-)$	RBW	$m_0 = 2709 \pm 4$, $\Gamma_0 = 117 \pm 13$
$D_{sJ}^*(2860)^-$	1	$m^2(\bar{D}^0K^-)$	RBW	See text
$D_{sJ}^*(2860)^-$	3	$m^2(\bar{D}^0K^-)$	RBW	See text
Nonresonant		$m^2(\bar{D}^0K^-)$	EFF	See text
$D_{s\,v}^{*-}$	1	$m^2(\bar{D}^0K^-)$	RBW	$m_0 = 2112.3 \pm 0.5$, $\Gamma_0 = 1.9$
$D_{s0\,v}^*(2317)^-$	0	$m^2(\bar{D}^0K^-)$	RBW	$m_0 = 2317.8 \pm 0.6$, $\Gamma_0 = 3.8$
B_v^{*+}	1	$m^2(\bar{D}^0\pi^+)$	RBW	$m_0 = 5325.2 \pm 0.4$, $\Gamma_0 = 0$

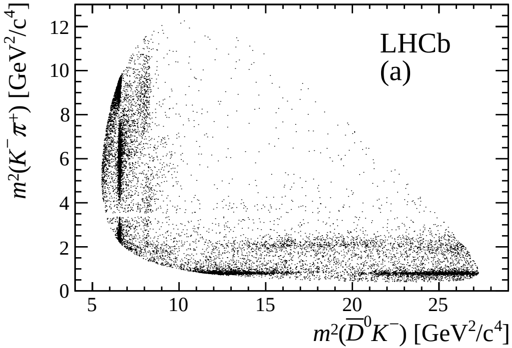

$D_{s2}(2573)$:

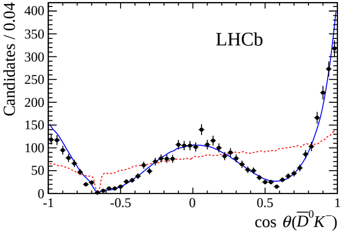

$D_{sJ}(2860)$:

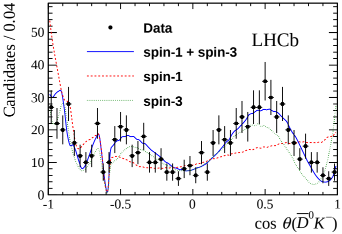

Resonance	Spin	Dalitz plot axis	Model	Parameters (MeV/c^2)
$\bar{K}^*(892)^0$	1	$m^2(K^-\pi^+)$	RBW	$m_0 = 895.81 \pm 0.19$, $\Gamma_0 = 47.4 \pm 0.6$
$\bar{K}^*(1410)^0$	1	$m^2(K^-\pi^+)$	RBW	$m_0 = 1414 \pm 15$, $\Gamma_0 = 232 \pm 21$
$\bar{K}_0^*(1430)^0$	0	$m^2(K^-\pi^+)$	LASS	See text
$\bar{K}_2^*(1430)^0$	2	$m^2(K^-\pi^+)$	RBW	$m_0 = 1432.4 \pm 1.3$, $\Gamma_0 = 109 \pm 5$
$\bar{K}^*(1680)^0$	1	$m^2(K^-\pi^+)$	RBW	$m_0 = 1717 \pm 27$, $\Gamma_0 = 322 \pm 110$
$\bar{K}_0^*(1950)^0$	0	$m^2(K^-\pi^+)$	RBW	$m_0 = 1945 \pm 22$, $\Gamma_0 = 201 \pm 90$
$D_{s2}^*(2573)^-$	2	$m^2(\bar{D}^0K^-)$	RBW	See text
$D_{s1}^*(2700)^-$	1	$m^2(\bar{D}^0K^-)$	RBW	$m_0 = 2709 \pm 4$, $\Gamma_0 = 117 \pm 13$
$D_{sJ}^*(2860)^-$	1	$m^2(\bar{D}^0K^-)$	RBW	See text
$D_{sJ}^*(2860)^-$	3	$m^2(\bar{D}^0K^-)$	RBW	See text
Nonresonant		$m^2(\bar{D}^0K^-)$	EFF	See text
$D_{s\,v}^{*-}$	1	$m^2(\bar{D}^0K^-)$	RBW	$m_0 = 2112.3 \pm 0.5$, $\Gamma_0 = 1.9$
$D_{s0\,v}^*(2317)^-$	0	$m^2(\bar{D}^0K^-)$	RBW	$m_0 = 2317.8 \pm 0.6$, $\Gamma_0 = 3.8$
B_v^{*+}	1	$m^2(\bar{D}^0\pi^+)$	RBW	$m_0 = 5325.2 \pm 0.4$, $\Gamma_0 = 0$

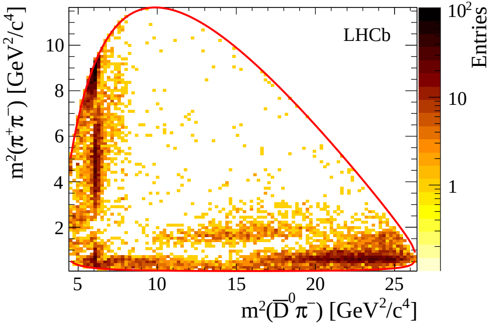

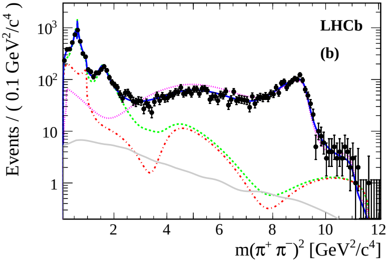

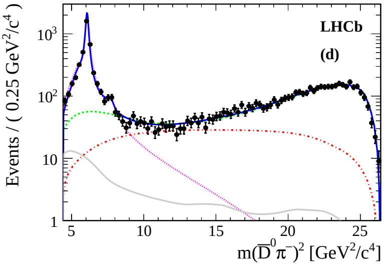

Resonance	Spin	Model	m_r (MeV/c^2)	Γ_0 (MeV)
$\bar{D}^0\pi^-$ P-wave	1	Eq. **??**	Floated	
$D_0^*(2400)^-$	0	RBW	Floated	
$D_2^*(2460)^-$	2	RBW	Floated	
$D_J^*(2760)^-$	3	RBW	Floated	
$\rho(770)$	1	GS	775.02 ± 0.35	149.59 ± 0.67
$\omega(782)$	1	Eq. **??**	781.91 ± 0.24	8.13 ± 0.45
$\rho(1450)$	1	GS	1493 ± 15	427 ± 31
$\rho(1700)$	1	GS	1861 ± 17	316 ± 26
$f_2(1270)$	2	RBW	1275.1 ± 1.2	$185.1\,^{+2.9}_{-2.4}$
$\pi\pi$ S-wave	0	K-matrix	See Sec. **??**	
$f_0(500)$	0	Eq. **??**	See Sec. **??**	
$f_0(980)$	0	Eq. **??**	See Sec. **??**	
$f_0(2020)$	0	RBW	1992 ± 16	442 ± 60
Nonresonant	0	Eq. **??**	See Sec. **??**	

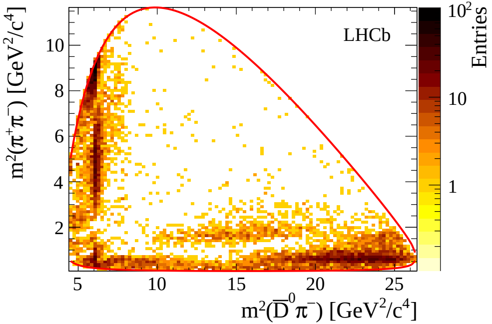

$D_J^*(2760)$:

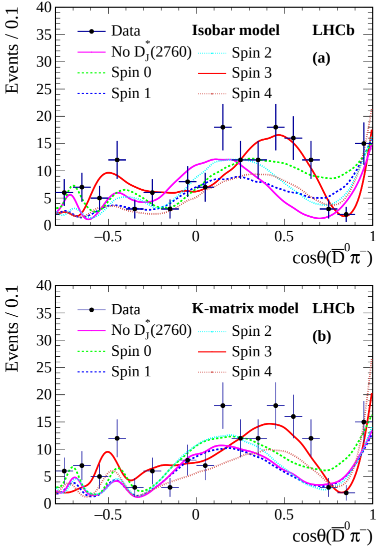

Resonance	Spin	Model	m_r (MeV/c^2)	Γ_0 (MeV)
$\bar{D}^0\pi^-$ P-wave	1	Eq. ??	Floated	
$D_0^*(2400)^-$	0	RBW	Floated	
$D_2^*(2460)^-$	2	RBW	Floated	
$D_J^*(2760)^-$	3	RBW	Floated	
$\rho(770)$	1	GS	775.02 ± 0.35	149.59 ± 0.67
$\omega(782)$	1	Eq. ??	781.91 ± 0.24	8.13 ± 0.45
$\rho(1450)$	1	GS	1493 ± 15	427 ± 31
$\rho(1700)$	1	GS	1861 ± 17	316 ± 26
$f_2(1270)$	2	RBW	1275.1 ± 1.2	$185.1\,^{+\,2.9}_{-\,2.4}$
$\pi\pi$ S-wave	0	K-matrix	See Sec. ??	
$f_0(500)$	0	Eq. ??	See Sec. ??	
$f_0(980)$	0	Eq. ??	See Sec. ??	
$f_0(2020)$	0	RBW	1992 ± 16	442 ± 60
Nonresonant	0	Eq. ??	See Sec. ??	

Dalitz plot anlayses: $B^0 \to \bar{D}^0\pi^+\pi^-$ [PRD 92 (2015) 032002]

Comparison of isobar and K-matrix for spin-0 $\pi^+\pi^-$ wave

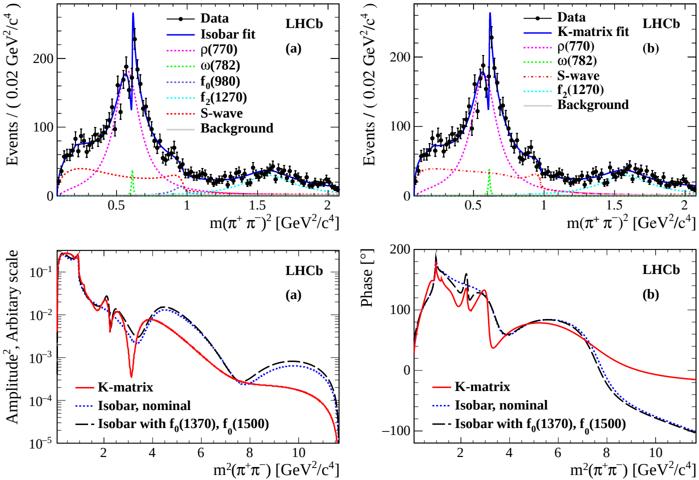

There are differences, but the effect on the fit quality is small.

Model-independent approaches: Legendre moments

Allow to investigate the helicity structure as a function of m^2 *without* performing a fit. Use the fact that partial wave with spin J is a Legendre polynomial $P_J(\cos\theta_{\rm hel})$.

Weight events as functions of helicity:

$$w_i = P_L(\cos\theta_{\rm hel})$$

Partial waves with spins up to J give moments up to $2J$ in the event density.

If we are limited to S, P and D waves:

$$\begin{aligned}
\langle P_0\rangle &= |h_0|^2 + |h_1|^2 + |h_2|^2 \\
\langle P_1\rangle &= \frac{2}{\sqrt{3}}|h_0||h_1|\cos\delta_{01} + \frac{4}{\sqrt{15}}|h_1||h_2|\cos\delta_{12} \\
\langle P_2\rangle &= \frac{2}{\sqrt{5}}|h_0||h_2|\cos\delta_{02} + \frac{2}{5}|h_1|^2 + \frac{2}{7}|h_2|^2 \\
\langle P_3\rangle &= \frac{6}{7}\sqrt{\frac{3}{5}}|h_1||h_2|\cos\delta_{12} \\
\langle P_4\rangle &= \frac{2}{7}|h_2|^2
\end{aligned}$$

Resonances only in one channel: $D^+\pi^-$: ideal for Legendre polynomial approach

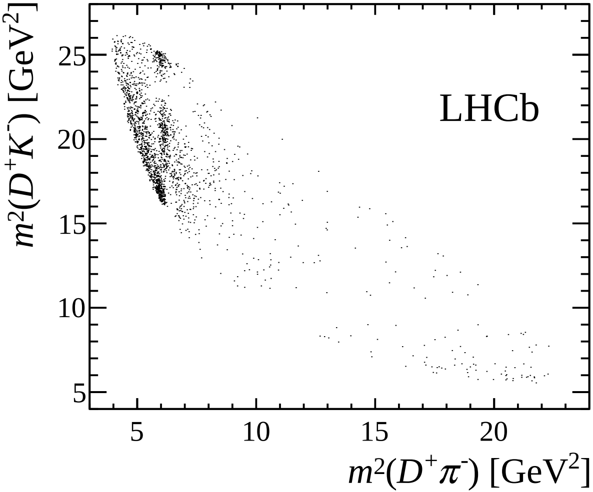

Consider contributions up to spin-3:

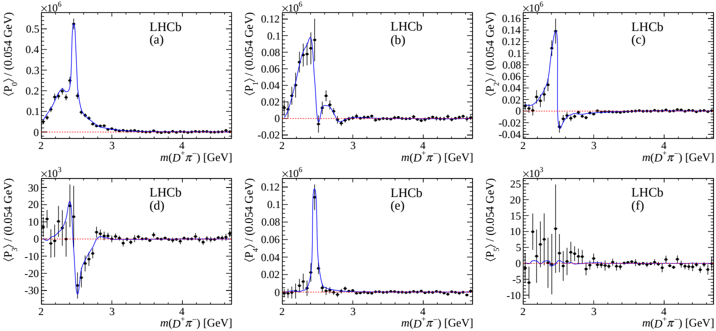

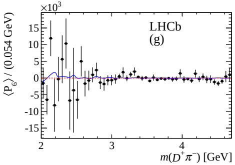

- Moments 6 and 7 consistent with 0: no evidence for PW with spin-3.
- Spin-2 apparent in moment 4: single state $D_2^*(2460)$
- Moment 3 differs from 4: interference with spin-2 and broad spin-1
- Moments 1 and 3 differ again: interference of spin-1 and spin-0 (broad as well)

Resonances only in $D^+\pi^-$, but two identical pions in the final state: need to symmetrise the amplitude

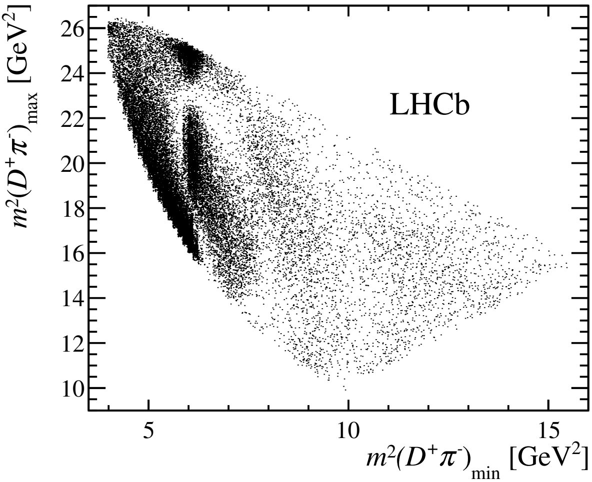

Legendre moments: $B^- \to D^+\pi^-\pi^-$ [arXiv:1608.01289]

Consider contributions up to spin-3:

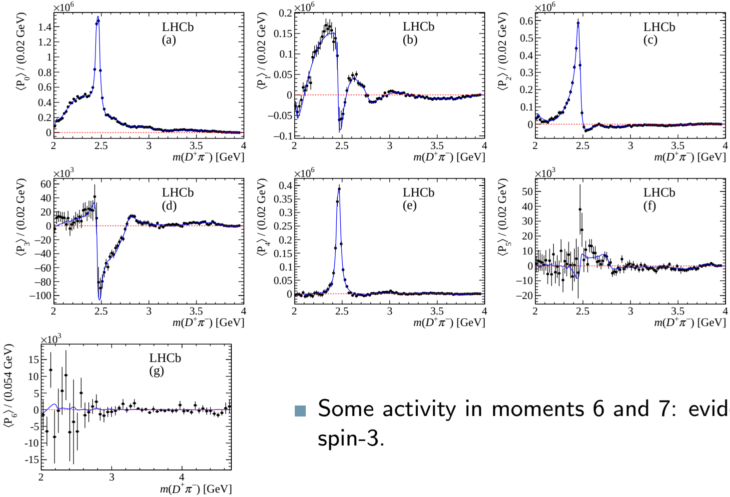

- Some activity in moments 6 and 7: evidence for PW with spin-3.

Model-independent S-wave: $B^- \to D^+\pi^-\pi^-$ [arXiv:1608.01289]

Large data sample allows to describe the S-wave by a model-independent spline-interpolated shape.
$Re(A)$ and $Im(A)$ in each node are fitted.
Interference with higher-spin waves provides information about the phase.

Resonance	Spin	Model	Parameters
$D_2^*(2460)^0$	2	RBW	Determined from data (see Table **??**)
$D_1^*(2680)^0$	1	RBW	
$D_3^*(2760)^0$	3	RBW	
$D_2^*(3000)^0$	2	RBW	
$D_v^*(2007)^0$	1	RBW	$m = 2006.98 \pm 0.15\,\mathrm{MeV},\ \Gamma = 2.1\,\mathrm{MeV}$
B_v^{*0}	1	RBW	$m = 5325.2 \pm 0.4\,\mathrm{MeV},\ \Gamma = 0.0\,\mathrm{MeV}$
Total S-wave	0	MIPW	See text

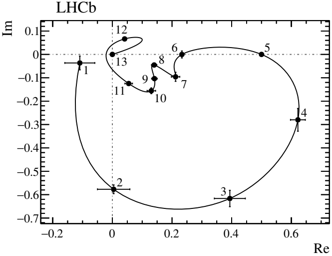

Phase rotation due to resonant $D^*(2400)$ state.

$D^0 \to K_S^0\pi^+\pi^-$ Dalitz plot

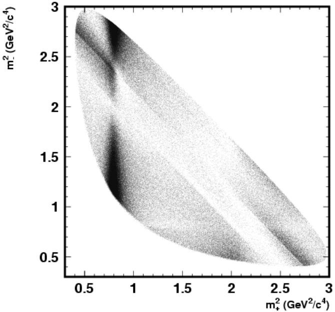

The amplitude contains $O(10)$ resonant contributions in $K\pi$ (K^*, K_0^*, K_2^*) and $\pi\pi$ (ρ, ω, f_0, f_2 etc.) channels

$D^0 \to K_S^0\pi^+\pi^-$ decay is unique to combine the following properties:

- High branching fraction.
- Rich resonance structure $\Rightarrow$ significant phase variations across the phase space.

Can be used to effectively measure the properties of $D^0 - \overline{D}^0$ admixture which appears in a few measurements:

- γ measurement in $B \to DK$
- D^0 mixing and CP violation
- β measurement in $B^0 \to D\pi^0$.

CKM angle γ: $D \to K_S^0\pi^+\pi^-$ decay from $B \to DK$

Measures CKM phase γ at tree level, $\Rightarrow$ SM reference point.

$B^- \to D^0 K^-$:

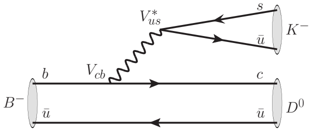

$A \sim V_{cb}V_{us}^* \sim A\lambda^3$

+

$B^- \to \overline{D}^0 K^-$:

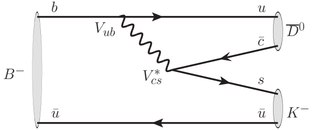

$A \sim V_{ub}V_{cs}^* \sim A\lambda^3(\rho - i\eta)$

If D^0 and $\overline{D}^0$ decay into the same final state: $|\tilde{D}\rangle = |D^0\rangle + r_B e^{\pm i\gamma + i\delta_B}|\overline{D}^0\rangle$ for $B^\pm$

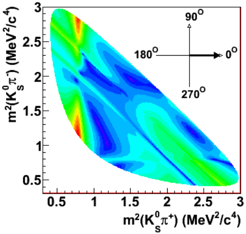

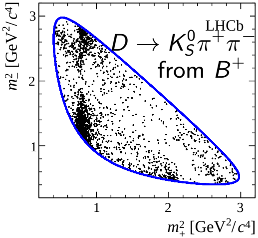

2D kinematic distribution of $D \to K_S^0\pi^+\pi^-$ from $B^\pm \to DK^\pm$

$p_\pm(m_+^2, m_-^2) = |A_D + r_B e^{\pm i\gamma + i\delta}\,\overline{A}_D|^2$

where A_D is known from flavour-specific $D^* \to D^0\pi$ decays

Obtain unknown r_B, δ_B and γ.

Measures CKM phase γ at tree level, $\Rightarrow$ SM reference point.

$B^- \to D^0 K^-$:

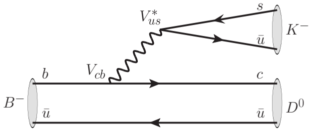

$A \sim V_{cb}V_{us}^* \sim A\lambda^3$

$+$

$B^- \to \overline{D}^0 K^-$:

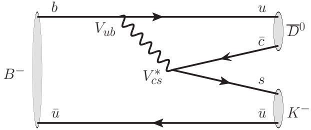

$A \sim V_{ub}V_{cs}^* \sim A\lambda^3(\rho - i\eta)$

If D^0 and $\overline{D}^0$ decay into the same final state: $|\tilde{D}\rangle = |D^0\rangle + r_B e^{\pm i\gamma + i\delta_B}|\overline{D}^0\rangle$ for $B^\pm$

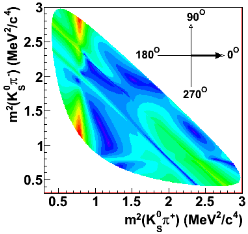

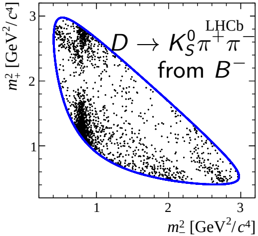

2D kinematic distribution of $D \to K_S^0\pi^+\pi^-$ from $B^\pm \to DK^\pm$

$p_\pm(m_+^2, m_-^2) = |A_D + r_B e^{\pm i\gamma + i\delta}\,\overline{A}_D|^2$

where A_D is known from flavour-specific $D^* \to D^0\pi$ decays

Obtain unknown r_B, δ_B and γ.

Part II

Multidimensional amplitude analyses

to be continued...